ACS OMEGA

http://pubs.acs.org/journal/acsodf

Article

Estimating Lost Gas Content for Shales Considering Real Boundary Conditions during the Core Recovery Process

Lingjie Yu, Yuling Tan,* Ming Fan, Ershe Xu, Guanglei Cui, and Zhejun Pan*

Cite This: *ACS Omega* 2022, 7, 21246−21254

Read Online

ACCESS | Metrics & More | Article Recommendations

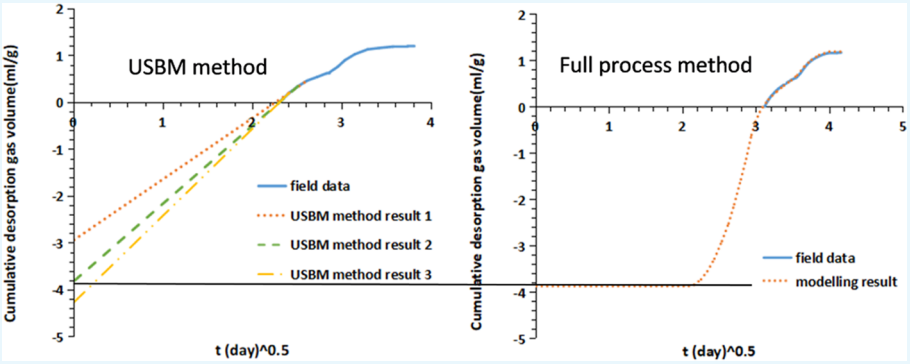

ABSTRACT: Shale gas has become an important natural gas resource in recent years as the conventional oil and gas resources are depleting. Shale gas content is one of the most important parameters for reserve calculation and sweet-spot prediction. The traditional core recovery method is widely used to determine gas content. However, the estimation of lost gas content is the main factor of error and difficulty. Large errors and uncertainties occur when using the widely used methods, such as the United States Bureau of Mines (USBM) method. Hence, a more accurate method is required. In this work, a full-process model is developed in COMSOL Multiphysics to describe the lost gas with time during the core recovery process as well as the desorption stage after the core is covered. In this method, by setting the initial gas pressure and flow parameters and matching the desorbed gas volume and considering variable diffusivity with respect to temperature, the initial gas content and the gas lost with respect to time are calculated. Overall, 10 field data are tested using this full-process model, and the USBM method is also applied to compare the results. It is found that if the ratio of lost gas volume estimated using the USBM method to the desorbed gas volume of the field data is lower than 2.0, the USBM method underestimates the lost gas compared to the full-process method; if the ratio is about 2.0, the results from the USBM and the full-process methods are comparable; and if the ratio is close to 3.0, the USBM method tends to overestimate the lost gas. The modeling results indicate that this proposed full-process method is more theoretically sound than the USBM method, which has high uncertainties depending on the number of desorbed gas data points used. Nevertheless, this proposed method requires a large number of parameters, leading to the difficulty in finding true parameters. Therefore, an optimization algorithm is required. In summary, this study provides theoretical support and a mathematical model for the inversion calculation of lost gas during shale core recovery. It is helpful to evaluate the resource potential and development economics of shale gas more accurately.

1. INTRODUCTION

As the world is shifting to a low carbon economy, there is a need to reduce greenhouse gas emissions.[1,2] The global demand for natural gas, which is a less carbon-intensive fossil fuel than coal and oil, has increased steadily over the last decades. While the reserves for the conventional natural gas decline in many gas-producing countries, unconventional natural gas, especially shale gas, has become an important natural gas resource in recent years in North America and China.[3] Gas content is an important parameter for shale resource calculation, gas-bearing evaluation, sweet-spot selection, reserve prediction, etc. Therefore, studying shale gas content helps to better guide the exploration and development of shale gas.[4,5] Gas content can be analyzed qualitatively or quantitatively by a number of methods, including the isothermal adsorption method, the gas logging interpretation

Received: April 17, 2022
Accepted: May 26, 2022
Published: June 10, 2022

method, linear fitting, seismic inversion, and the field desorption method.[6−8] The isothermal adsorption method can indirectly calculate gas content; however, temperature correction is required when the difference between experimental and stratum temperature is large.[5] The gas logging interpretation method is applicable to a small scale and only for the calculation of gas content in a single shale well, and it cannot obtain the evolution characteristics of gas content in the region.[8] The accuracy of linear fitting and seismic inversion is restricted by the measured value of gas content and the accuracy of seismic data.[8] The field desorption method is the most direct method to quantitatively determine the gas content of shale.[7,9,10] The operating procedure of the field desorption method is to use the coring tool to drill the core from the formation and lift it to the surface. Then, the core is sealed in the desorption canister and the desorbed gas volume is measured by a desorption apparatus, the residual gas content is measured by a ball mill, and the lost gas content is calculated by desorption data. The total shale gas volume is obtained by adding the desorbed gas volume, residual gas volume, and lost gas volume,[7,9] as illustrated in Figure 1.[11]

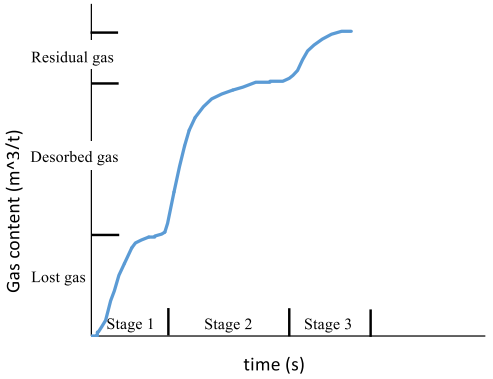

Figure 1. Gas content by the desorption method[11] (stage 1 represents the core recovering process, stage 2 represents the desorption process in the desorption canister, and stage 3 represents the residual gas measuring process).

During shale gas content testing, core samples are drilled from the reservoir and brought to the surface by ropes. Gas is lost as the core is transported from the formation to the surface. The lost gas cannot be measured directly and needs to be estimated by models.[12,13] The estimation of lost gas content is the main factor of error and difficulty in the determination of gas content.[4] At present, the methods of evaluating shale lost gas content include the United States Bureau of Mines (USBM) method,[14,15] the Smith−Williams method,[16,17] the polynomial function method,[18] the Amoco curve fit method,[19,20] the desorption critical time point method,[12] and the improved direct method.[21] For example, Lu[22] et al. proposed a three-parameter model, which could offer a more accurate prediction for estimating the lost gas during the retrieval process of coals than the USBM method.

Among the above methods, the USBM method and its modified versions are more commonly adopted because of their simplicity and easiness to apply. However, the USBM method is proposed for coal gas,[12,14,23−26] which is also a major unconventional gas resource in countries such as China.[27] In this method for coal gas, the lost gas is estimated from the early desorbed gas measurement, assuming that the loss of gas is proportional to the square root of time.[14] Besides, it assumes that the initial desorption time of the gas is half the time that it takes from the beginning of the lifting to the core reaching the ground.[7] This is suitable for coal because the coal seam is generally shallow, and the loss of gas is relatively small. However, shale gas reservoirs are typically deep[28] and the core recovery process takes much longer time than coal,[29] typically more than 10 h for shales and less than 1 h for coals. Therefore, the proportional relationship between the desorbed gas volume and the square root of time is no longer valid. Meantime, taking the definition of the above initial desorption time also has big problems in the estimation of lost gas from shale because the time of initial desorption is closely related to the pressure of the core and the density of the drilling fluid. To evaluate the lost gas and the gas-in-place in shales, Lu[30] et al. proposed a nonisothermal flow model, considering that the thermal effect plays a key role. However, the mathematical model in Lu et al.[30] contains a number of model parameters. It needs to deal with strong nonlinearity and often generates a set of nonunique solutions when using that method, which brings great uncertainty, randomness, and complexity to the estimation of lost gas.

Based on the above analyses, this work aims to provide theoretical support and a mathematical model for the inversion calculation of lost gas from the shale core recovering process by adopting a physical process more in line with the on-site coring process. First, this work establishes a full-process model for the recovery of lost gas. By changing the parameters such as initial pressure and diffusivity, the relationship between lost gas and time in the process of core recovering and after the sample reaching the ground is reconstructed. Then, the calculated desorbed gas amount with time and that measured on site are compared and matched to estimate the lost gas. The mathematical model is calculated in COMSOL Multiphysics software. Finally, the calculation of lost gas is discussed with the actual field data.

2. METHODS

2.1. Core Recovery Process. According to literature description and field operation, the full shale core recovery and gas content determination procedure steps are as follows:[23,31]

(1) After the core is drilled, it begins to leave the formation. At this time, gas does not desorb because the pressure of the drilling fluid in the wellbore is higher than the pressure of the gas in the core. Moreover, due to the circulation of the drilling fluid, the core slowly heats to a temperature close to the drilling fluid.

(2) The core is pulled to a certain position in the wellbore and the gas begins to desorb. At this point, the internal pressure of the core is equal to the pressure generated by the drilling fluid at this location in the wellbore. Then, the pressure boundary condition on the core sample continues to change as the core is pulled to the surface.

(3) After the core reaches the surface and before the core is transferred to the desorption canister, desorption continues and the core is subjected to atmospheric pressure. To accurately measure gas content, this part of the time should be as short as possible.

(4) After the core is transferred to the desorption canister, the amount of desorbed gas is recorded with time. At this stage, the temperature on the core is the water bath temperature and the pressure is atmospheric pressure.

https://doi.org/10.1021/acsomega.2c02397
ACS Omega 2022, 7, 21246−21254

(5) To speed up the desorption rate, the desorption canister temperature is increased to the second stage desorption temperature. The amount of gas desorbed is still recovered with time and the pressure on the boundary is still atmospheric pressure.

It should be noted that the desorption temperature for coal gas content measurement is often controlled at reservoir temperature; however, two stages of desorption temperature are often adopted for shale gas desorption.[32] The above procedure can be described using the mathematical equations described in the following section.

2.2. Full-Process Mathematical Model. When the USBM method is applied to shale gas, it will produce large errors and uncertainties due to the long core recovery process. Therefore, this work established a full-process model to estimate the lost gas during shale gas content measurement. The shale samples used for numerical simulation of lost gas recovery are cylindrical. The sample radius and height can be adjusted according to the actual size of the sample. Neglecting the short time after the core reaches the surface and before the core is transferred to the desorption canister, the time of the whole process of desorption is divided into four stages:

(a) From drilling-off to the beginning of gas desorption: $t = 0 \rightarrow t = t_{des}$.
(b) From the beginning of gas desorption to the sample arriving at the wellhead: $t = t_{des} \rightarrow t = t_{surface}$.
(c) From sample arriving at the wellhead to applying a second desorption temperature: $t = t_{surface} \rightarrow t = t_1$.
(d) From applying a second desorption temperature to ending of desorption: $t = t_1 \rightarrow t = t_{over}$.

In these four stages, the boundary pressure and temperature of the core change with time. The boundary pressure changes as follows

$$p_{out} = \begin{cases} p_0, (t \le t_{des}) \\ p_{mud} - (p_{mud} - p_a)\dfrac{t}{t_{surface}}, (t_{des} < t \le t_{surface}) \\ p_a, (t > t_{surface}) \end{cases} \tag{1}$$

where p_0 is initial gas pressure, p_a is the standard atmosphere, and $p_{mud} = \rho_{mud}gH$ is the mud pressure at depth H in the well. Note that the rate of core lifting is assumed constant in this work but can be adjusted according to the actual lifting process.

When the mud pressure on the core is higher than the desorption pressure, the gas in the core does not desorb and the boundary pressure is the original pressure in the core. When the mud pressure on the core is the same as the desorption pressure, the gas in the sample begins to desorb. The time when gas begins to desorb is as follows

$$t_{des} = \frac{p_{mud} - p_0}{p_{mud} - p_a} t_{surface} \tag{2}$$

The temperature of the sample is

$$T = \begin{cases} T_{mud} (t \le t_{surface}) \\ T_1 \quad (t_{surface} < t < t_1) \\ T_2 \quad (t > t_1) \end{cases} \tag{3}$$

where T_{mud} is the mud temperature, T_1 is the first desorption temperature, and T_2 is the second desorption temperature.

According to the results in the literature,[33,34] the pore structure of shales can be regarded as dual porosity, in which large and small pores both contain adsorbed gas and free gas. The permeability in the fracture system is typically two to three orders of magnitude higher than in the matrix, which can be measured perpendicular to the bedding direction.[35] We derive diffusivity and mass balance equations in macropore and micropore as follows (see Appendix A)

The gas diffusivity in macropore is

$$D_{mac} = D_{mac0}\left(1 + b\frac{T - T_{mud}}{T_{mud}}\right)e^{\alpha(p_{mac} - p_0)} \tag{4}$$

where D_{mac0} is gas diffusivity in the macropore in the initial state.

The mass balance equation in the macropore is[36]

$$\frac{\partial(m_{mac-ads} + m_{mac-free})}{\partial t} + \nabla \cdot J_{mac} = Q \tag{5}$$

where J_{mac} is the gas flow flux in the macropore

$$J_{mac} = -D_{mac}\left(\frac{\phi_{mac}\rho_{ga}}{p_a Z_{mac}} + \rho_{ga}\rho_{shale}\frac{V_{mac-L}p_{mac}}{(P_{mac-L} + p_{mac})^2}\right)\nabla p_{mac} \tag{6}$$

Q is the commutative term of the macropore and the micropore.

The gas diffusivity in the micropore is

$$D_{mic} = D_{mic0}\sqrt{\frac{T}{T_{mud}}} \tag{7}$$

where D_{mic0} is gas diffusivity in the micropore in the initial state.

The mass balance equation in the micropore is

$$\frac{\partial(m_{mic-ads} + m_{mic-free})}{\partial t} + \nabla \cdot J_{mic} = Q \tag{8}$$

where J_{mic} is the gas flow flux in the micropore

$$J_{mic} = -D_{mic}\left(\frac{\phi_{mic}\rho_{ga}}{p_a Z_{mic}} + \rho_{ga}\rho_{shale}\frac{V_{mic-L}p_{mic}}{(P_{mic-L} + p_{mic})^2}\right)\nabla p_{mic} \tag{9}$$

Q is the commutative term of the macropore and the micropore

$$Q = \frac{\alpha_{mic}D_{mic}\phi_{mic}}{p_a Z_{mic}}\frac{p_{mic}}{p_a}\rho_{ga}(p_{mac} - p_{mic}) + \rho_{ga}\rho_{shale}\alpha_{mic}D_{mic}\left(\frac{V_{mac-L}p_{mac}}{P_{mac-L} + p_{mac}} - \frac{V_{mic-L}p_{mic}}{P_{mic-L} + p_{mic}}\right) \tag{10}$$

where α_{mic} is the shape factor of the micropore.

This mathematical model is calculated by COMSOL Multiphysics simulation software. Based on the finite element method, real physical phenomena are simulated by solving partial differential equations (single field) or partial differential equations (multiple fields). The advantage of COMSOL Multiphysics lies in the coupling of multiple physical fields. The essence of multiple physical fields is a system of partial

https://doi.org/10.1021/acsomega.2c02397
ACS Omega 2022, 7, 21246−21254

differential equations. Therefore, as long as it is a physical phenomenon that can be described by a system of partial differential equations, COMSOL Multiphysics can be used to well calculate and simulate. Figure 2 illustrates the flowchart of

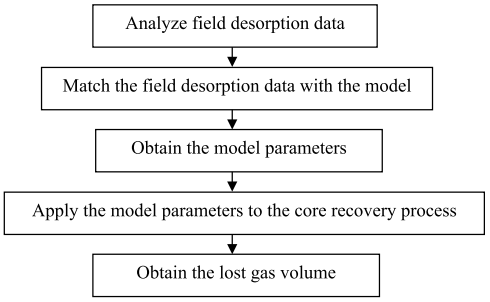

Figure 2. Work flowchart of the full-process method.

the proposed full-process method. First, the field desorption data are analyzed and processed; then, the model is applied to best fit the field desorption data to obtain the model parameters. Next, these model parameters are applied to the core recovery process to obtain the amount of lost gas. Finally, the results are plotted.

3. RESULTS AND DISCUSSION

The method of lost gas recovery is to match the model result with the measured field desorption data after the core reaches the ground, and then to obtain the lost gas volume. In this part, the lost gas recovery calculation based on 10 sets of field data is presented. We compared the modeling results using the USBM method and the full-process method proposed in this work and discussed the influencing parameters for the full-process method.

3.1. Calculation of Lost Gas Recovery Based on Field Data. Table 1 presents the estimated volume of lost gas for 10 samples using the USBM method and the full-process method based on field data of desorbed gas measurement. The results using USBM depend on the measured data points used in the calculation, as shown in Figure 3. Due to the curvature of the

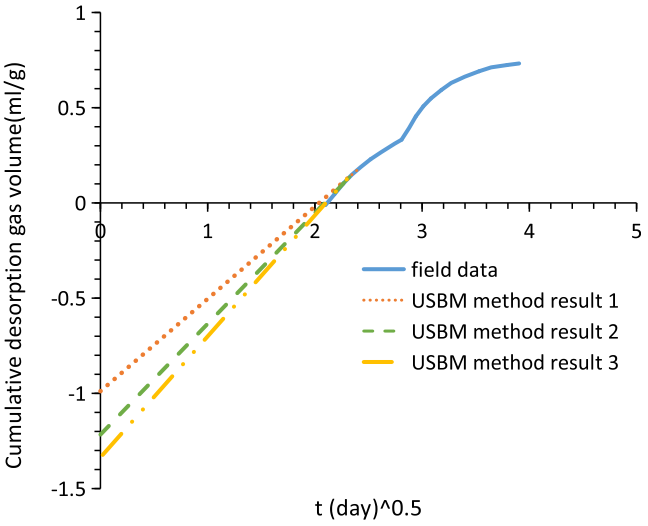

Figure 3. Modeling result using the USBM method for #2.

desorbed gas data with respect to the square root of time, the estimated lost gas tends to be larger if fewer data points are used and vice versa. Therefore, it is difficult to obtain a fixed value using the USBM method, and a range of values are more reasonable, as listed in Table 1. Moreover, the difference in lost gas between the two methods is also listed in Table 1. The difference is taken as the ratio of the USBM results to the result of the full-process method. If the differences are from less than 1 to more than 1, it means that the result of the full-process method is within the range of that using the USBM method. If the differences are always less than 1, it means that the result of the full-process method is higher than that using the USBM method and vice versa.

Table 1. Modeling Result of Lost Gas

well no.	sample weight (g)	sample size (m)	desorbed gas volume (mL/g)	lost gas (USBM method) (mL/g)	lost gas (full-process method) (mL/g)	ratio	difference
#1	3737	R: 0.05 L: 0.18	0.54	1.02−1.31	1.23	1.89−2.43	0.83−1.07
#2	3806	R: 0.05 L: 0.185	0.79	1.19−1.48	2.05	1.51−1.87	0.58−0.72
#3	3340	R: 0.05 L: 0.162	0.60	0.90−1.22	1.38	1.50−2.03	0.65−0.88
#4	3473	R: 0.05 L: 0.17	0.72	1.79−2.19	1.61	2.49−3.04	1.11−1.36
#5	3523	R: 0.05 L: 0.17	1.14	2.32−3.25	2.55	2.04−2.85	0.91−1.27
#6	3745	R: 0.05 L: 0.182	0.24	0.69−0.86	0.69	2.88−3.58	1.00−1.26
#7	3396	R: 0.05 L: 0.166	0.44	1.16−1.47	1.18	2.64−3.34	0.98−1.25
#8	3503	R: 0.05 L: 0.171	0.86	2.51−2.78	2.34	2.92−3.23	1.07−1.19
#9	4774	R: 0.05 L: 0.233	0.65	1.70−1.97	2.11	2.62−3.03	0.81−0.93
#10	4086	R: 0.05 L: 0.2	1.22	3.79−4.46	3.92	3.11−3.66	0.97−1.14

https://doi.org/10.1021/acsomega.2c02397
ACS Omega 2022, 7, 21246−21254

The ratio of lost gas volume using the USBM method to the desorbed gas volume of the field data is also listed in Table 1. This ratio is to illustrate the difficulty of using the measured desorbed gas volume to estimate the lost gas. A small ratio means that the lost gas volume is less significant compared to the desorbed gas volume and can be more accurate to estimate; for instance, this ratio is often only 0.2 for coal gas cases. However, the ratio is at least 1.5 and often more than 3.0 in this work, as can be seen from Table 1, indicating that the estimated lost gas would be much higher than the desorbed gas and thus show a larger error in lost gas estimation. It is found that samples #2 and #3 have a lower ratio (typically less than 2.0) than other wells, and the difference between the two methods is less than 1.0, suggesting that the USBM method could underestimate the lost gas volume. If the ratio is around 2.0, the differences between the two methods are from less than 1.0 to more than 1.0 (Samples #1, 5, 7), suggesting that the lost gas estimate using both methods could be comparable. If the ratio is close to 3.0, the difference tends to be more than 1.0 (Samples #4, 6, 8, 10), suggesting that the USBM method will overestimate the lost gas compared to that using the full-process method.

To display the results more visually, the modeling results for two wells, well #2 and #10, are plotted in Figures 3−6 as illustrations. It should be noted that the X coordinate is the square root of time. It should be also noted that time zero for the two methods is different. For the following figures for the full-process method, the time when the core leaves the reservoir is zero, which is different from the zero time in figures obtained using the USBM method.

Figure 3 shows the modeling result using USBM method for sample #2. The desorbed gas volume after the core reaches the ground is about 0.79 mL/g. The data used by the USBM method (straight line) have a good linearity. R^2 (coefficient of determination) is 0.9995 for result 2 and the estimated lost gas is about 1.31 mL/g. As shown in Figure 3, if more or less desorption data points are used by the USBM method, the estimated volume of lost gas will become smaller or larger, without sacrificing much of the linearity of fitting (results 1 and 3). The modeling result using the full-process method for sample #2 is presented in Figure 4. The fitting of desorption data under the first desorption temperature has better agreement with the field data than the second desorption temperature. The volume of lost gas obtained is about 2.05 mL/g. The result using the full-process method is higher than that using the USBM method.

The field data of sample #10 show a relatively higher desorbed gas volume at about 1.22 mL/g, as shown in Figure 5. The calculated volume of lost gas is almost 3.79 mL/g using the USBM method (results 2). Result 1 using the USBM method also has good linearity, with R^2 of 0.994. It can also be seen from Figure 5, if more desorption data points are used by the USBM method, the estimated volume of lost gas will become smaller, and the linearity of fitting will become slightly worse and vice versa. Moreover, the ratio of lost gas volume using the USBM method to desorption gas volume of field data is high at about 3.0. Figure 6 shows the modeling result for sample #10 using the full-process model. It can be seen that the fitting result of desorption data under the first desorption and the second desorption temperature are both in good agreement with the field data. The volume of the lost gas

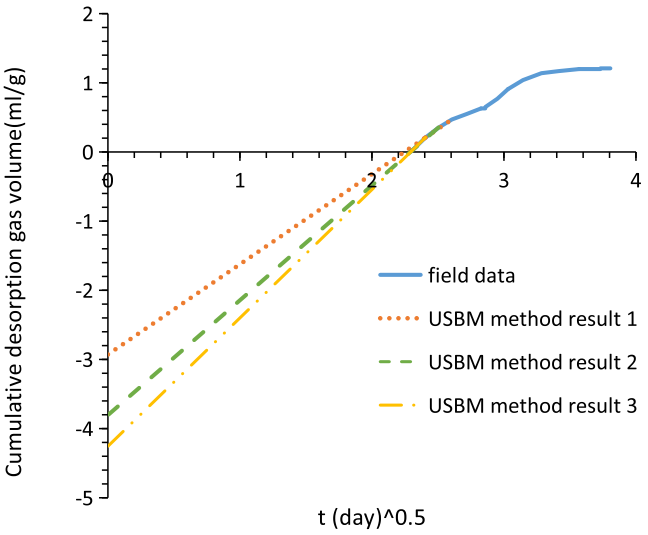

Figure 5. Modeling result using the USBM method for #10.

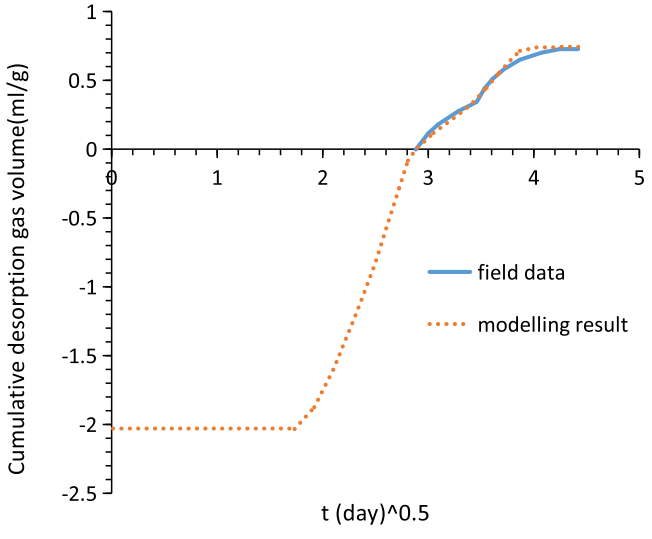

Figure 4. Modeling result using the full-process method for #2.

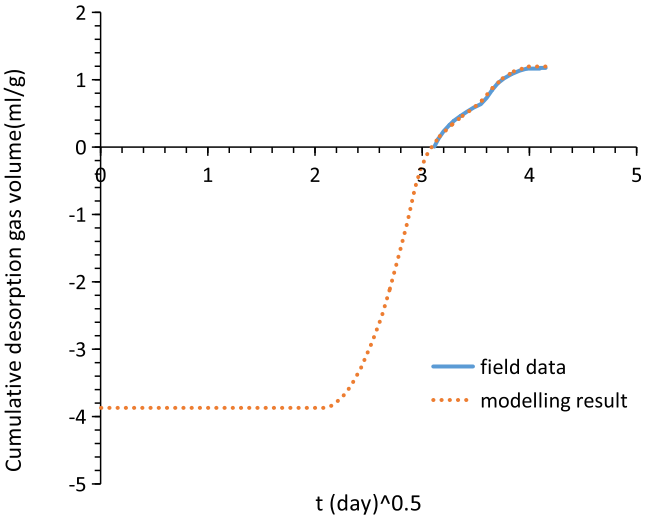

Figure 6. Modeling result using the full-process method for #10.

https://doi.org/10.1021/acsomega.2c02397
ACS Omega 2022, 7, 21246−21254

obtained is about 3.92 mL/g. This result is well within the results using the USBM method for this sample.

It can be seen from the above results that the value of the lost gas obtained using the USBM method depends on the number of points used from the desorption data. The USBM method assumes that gas desorption at early time is linear to the square root of time; however, this is not valid for the shale gas cases. Meantime, others have also proposed methods such as polynomial fitting, which can fit the desorption data well. Nevertheless, these methods are purely empirical and lack theoretical background. Therefore, these methods are not applicable. This proposed method and any similar method, which consider the gas flow behavior and boundary conditions, can estimate the lost gas with more certainty. Moreover, the relationship between the lost gas and time can also be obtained using the full-process method.

3.2. Influence of Parameters. In this full-process method, the flow parameters, especially the gas diffusivities, are critical in the estimation of lost gas. In this part, the influence of the initial gas diffusivity in the micropore (D_{mic0}) and the initial gas diffusivity in the macropore (D_{mac0}) on the process of gas desorption are studied. The influence of D_{mic0} is presented in Figure 7. The values of D_{mic0} used in the simulation are 0.5×10^{-4}, 1.1×10^{-4}, and 2.2×10^{-4} m^2/s, respectively. It can be seen that changing D_{mic0} will only impact the process of (c) and (d) described in Section 2.1, indicating that D_{mic0} mainly influences the part of gas desorption on the ground. Increasing D_{mic0} leads to increasing estimated desorption velocity on the ground. The influence of D_{mac0} is presented in Figure 8. It can be seen that changing D_{mac0} will impact the total process of gas desorption. Increasing D_{mac0} leads to increasing estimated desorption velocity in the whole process. This is due to the fact that most of the gas is lost during the core recovery process for shales and the gas left in the core is mainly in the micropores when the core reaches the ground. Therefore, gas diffusivity in the micropore (D_{mic0}) has more impact on the desorbed gas fitting, while diffusivity in the macropore (D_{mac0}) controls the gas flow behavior during the whole process. Hence, these two parameters need to be fit accurately, especially D_{mac0} to accurately estimate the lost gas.

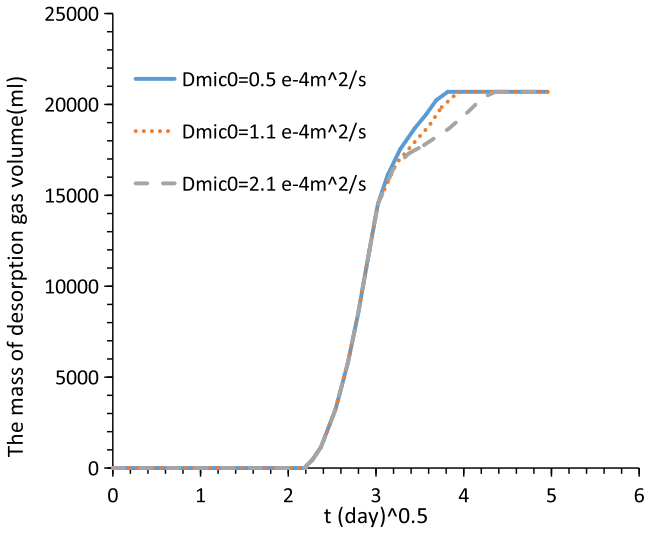

Figure 7. Influence of D_{mic0} on the process of gas desorption.

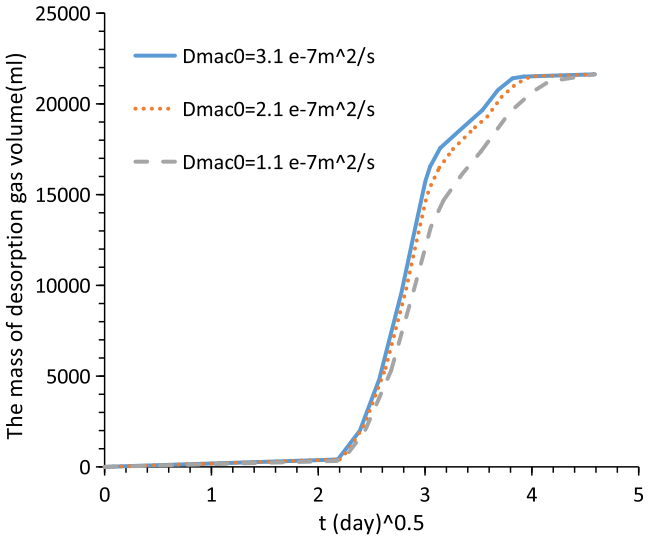

Figure 8. Influence of D_{mac0} on the process of gas desorption.

3.3. Problems of the Full-Process Method. The full-process method in this work can accurately describe the physical processes of gas loss but correct mathematical models and accurate estimation of physical parameters are required. Therefore, although the full-process method has more theoretical background than the USBM method, it needs to describe the flow physics in more detail. The most important parameters are the flow parameters and their relationship with pressure. Gas diffusivity changes with pressure and its relationship with pressure is hard to generalize.[34] This leads to difficulty in the more accurate estimation of lost gas and requires more experimental and theoretical study of gas diffusion in shales. Moreover, the geometric object in this full-process method is assumed to be a homogeneous cylindrical sample. However, shale is highly heterogeneous and anisotropic, thus gas flow in the core is also anisotropic.[37,38] Furthermore, it needs a lot of computation to fit the field data and then predict the lost gas. At present, this work does not involve the use of an optimization algorithm for parameter fitting. Hence, there is a lot of work in tuning the fitting parameters and there is still some error in the calculation of lost gas. It is preferred to have some of the flow parameters measured in the laboratory instead of being fitted to reduce the uncertainties and computational effort. Therefore, it is necessary to combine the optimization algorithm and consider more accurate gas diffusivity models and parameters to achieve more accurate results of the lost gas estimate.

4. SUMMARY AND CONCLUSIONS

This work aims to conduct mathematical modeling and provide theoretical support for the inversion calculation of shale lost gas. First, the full-process method of lost gas estimate for shale is established. Then, the mathematical model is calculated using COMSOL Multiphysics. Finally, taking the actual field data as examples, the calculation of lost gas is discussed. The below conclusions can be drawn:

(1) The proposed full-process method for shale lost gas is more theoretically sound. Diffusivity in this model is not constant but varies with temperature. In the part of desorption gas after core recovery, the modeling result is in good agreement with field data. Using the full-process

https://doi.org/10.1021/acsomega.2c02397
ACS Omega 2022, 7, 21246−21254

method, the relationship between the lost gas and time can be known.

(2) A large number of modeling parameters are required, leading to the difficulties to tune the model. Therefore, an optimization algorithm is required to make the calculation more convenient.

(3) If the ratio of lost gas volume using the USBM method to desorbed gas volume of field data is lower than 2.0, the USBM method underestimates the lost gas; if the ratio is about 2.0, the results from the USBM and the full-process methods are comparable; and if the ratio is close to 3.0, the USBM method tends to overestimate the lost gas.

As most of the core recovery practices do not apply closed coring technology due to its high cost, the lost gas estimate is key to the shale gas content measurement when using the conventional coring method. Therefore, the full-process method is preferred. However, due to the complex gas flow behavior in shales, more experimental and theoretical work is required to study the gas flow behavior. Moreover, an optimization algorithm should be applied to improve computation efficiency and accuracy.

APPENDIX A

The mass of adsorbed gas per unit volume in the macropore is[39]

$$m_{\mathrm{mac-ads}} = \rho_{\mathrm{ga}}\rho_{\mathrm{shale}}\frac{V_{\mathrm{mac-L}}p_{\mathrm{mac}}}{P_{\mathrm{mac-L}} + p_{\mathrm{mac}}} \tag{A-1}$$

where ρ_{ga} is the density of gas at standard conditions, ρ_{shale} is the density of shale, p_{mac} is the gas pressure in the macropore. and $V_{\mathrm{mac\text{-}L}}$ and $P_{\mathrm{mac\text{-}L}}$ are the Langmuir volume constant and the Langmuir pressure constant in the macropore, respectively.

In the initial state, the mass of adsorbed gas per unit volume in the macropore is

$$m_{\mathrm{mac-ads0}} = \rho_{\mathrm{ga}}\rho_{\mathrm{shale}}\frac{\mathrm{V}_{\mathrm{mac-L}}p_0}{P_{\mathrm{mac-L}} + p_0} \tag{A-2}$$

where p_0 is the initial gas pressure in the sample. Thus, the mass of lost adsorbed gas per unit volume in the macropore is $m_{\mathrm{mac\text{-}ads0}} - m_{\mathrm{mac\text{-}ads}}$.

The mass of free gas per unit volume in the macropore is[39]

$$m_{\mathrm{mac-free}} = \frac{p_{\mathrm{mac}}\rho_{\mathrm{ga}}\phi_{\mathrm{mac}}}{p_{\mathrm{a}}Z_{\mathrm{mac}}} \tag{A-3}$$

where ϕ_{mac} is the porosity of macropore, p_{a} is the standard atmosphere, and Z_{mac} is the gas compression factor of the macropore

$$Z_{\mathrm{mac}} = \begin{cases} Z_{\mathrm{mac-0}}(t \le \mathrm{t}_{\mathrm{surface}}) \\ Z_{\mathrm{mac-1}}(t_{\mathrm{surface}} < t \le t_1) \\ Z_{\mathrm{mac-2}}(t > t_1) \end{cases} \tag{A-4}$$

In the initial state, the mass of free gas per unit volume in the macropore is

$$m_{\mathrm{mac-free0}} = \frac{p_0\rho_{\mathrm{ga}}\phi_{\mathrm{mac}}}{p_{\mathrm{a}}Z_{\mathrm{mac-0}}} \tag{A-5}$$

Thus, the mass of lost free gas per unit volume in the macropore is $m_{\mathrm{mac\text{-}free0}} - m_{\mathrm{mac\text{-}free}}$.

The gas diffusivity in the macropore is

$$D_{\mathrm{mac}} = D_{\mathrm{mac0}}\left(1 + b\frac{T - T_{\mathrm{mud}}}{T_{\mathrm{mud}}}\right)e^{\alpha(p_{\mathrm{mac}} - p_0)} \tag{A-6}$$

where D_{mac0} is gas diffusivity in the macropore in the initial state.

The mass balance equation in the macropore is[36]

$$\frac{\partial(m_{\mathrm{mac-ads}} + m_{\mathrm{mac-free}})}{\partial t} + \nabla\cdot J_{\mathrm{mac}} = Q \tag{A-7}$$

whereJ_{mac} is the gas flow flux in the macropore

$$J_{\mathrm{mac}} = -D_{\mathrm{mac}}\left(\frac{\phi_{\mathrm{mac}}\rho_{\mathrm{ga}}}{p_{\mathrm{a}}Z_{\mathrm{mac}}} + \rho_{\mathrm{ga}}\rho_{\mathrm{shale}}\frac{V_{\mathrm{mac-L}}p_{\mathrm{mac}}}{(P_{\mathrm{mac-L}} + p_{\mathrm{mac}})^2}\right)\nabla p_{\mathrm{mac}} \tag{A-8}$$

Q is the commutative term of the macropore and the micropore.

For the micropore, the mass of the adsorbed gas per unit volume in the micropore is

$$m_{\mathrm{mic-ads}} = \rho_{\mathrm{ga}}\rho_{\mathrm{shale}}\frac{V_{\mathrm{mic-L}}p_{\mathrm{mic}}}{P_{\mathrm{mic-L}} + p_{\mathrm{mic}}} \tag{A-9}$$

where ρ_{ga} is the density of gas at standard conditions, ρ_{shale} is the density of shale, p_{mic} is the gas pressure in the micropore, and $V_{\mathrm{mic\text{-}L}}$ and $P_{\mathrm{mic\text{-}L}}$ are the Langmuir volume constant and the Langmuir pressure constant in the micropore, respectively.

In the initial state, the mass of the adsorbed gas per unit volume in the micropore is

$$m_{\mathrm{mic-ads0}} = \rho_{\mathrm{ga}}\rho_{\mathrm{shale}}\frac{V_{\mathrm{mic-L}}p_0}{P_{\mathrm{mic-L}} + p_0} \tag{A-10}$$

where p_0 is the initial gas pressure in the sample. Thus, the mass of the lost adsorbed gas per unit volume in the micropore is $m_{\mathrm{mic\text{-}ads0}} - m_{\mathrm{mic\text{-}ads}}$.

The mass of free gas per unit volume in the micropore is

$$m_{\mathrm{mic-free}} = \frac{p_{\mathrm{mic}}\rho_{\mathrm{ga}}\phi_{\mathrm{mic}}}{p_{\mathrm{a}}Z_{\mathrm{mic}}} \tag{A-11}$$

where ϕ_{mic} is the porosity of the micropore, p_{a} is the standard atmosphere, and Z_{mic} is the gas compression factor of the micropore

$$Z_{\mathrm{mic}} = \begin{cases} Z_{\mathrm{mic-0}}(t \le t_{\mathrm{surface}}) \\ Z_{\mathrm{mic-1}}(t_{\mathrm{surface}} < t \le t_1) \\ Z_{\mathrm{mic-2}}(t > t_1) \end{cases} \tag{A-12}$$

In the initial state, the mass of the free gas per unit volume of the micropore is

$$m_{\mathrm{mic-free0}} = \frac{p_0\rho_{\mathrm{ga}}\phi_{\mathrm{mic}}}{p_{\mathrm{a}}Z_{\mathrm{mic-0}}} \tag{A-13}$$

Thus, the mass of the lost free gas per unit volume in the micropore is $m_{\mathrm{mic\text{-}free0}} - m_{\mathrm{mic\text{-}free}}$.

The gas diffusivity in the micropore is

https://doi.org/10.1021/acsomega.2c02397
ACS Omega 2022, 7, 21246−21254

$$D_{mic} = D_{mic0}\sqrt{\frac{T}{T_{mud}}} \tag{A-14}$$

where D_{mic0} is the gas diffusivity in the micropore in the initial state.

The mass balance equation in the micropore is

$$\frac{\partial(m_{mic-ads} + m_{mic-free})}{\partial t} + \nabla \cdot J_{mic} = Q \tag{A-15}$$

where J_{mic} is the gas flow flux in the micropore

$$J_{mic} = -D_{mic}\left(\frac{\phi_{mic}\rho_{ga}}{p_a Z_{mic}} + \rho_{ga}\rho_{shale}\frac{V_{mic-L}p_{mic}}{(P_{mic-L} + p_{mic})^2}\right)\nabla p_{mic} \tag{A-16}$$

Q is the commutative term of the macropore and the micropore

$$Q = \frac{\alpha_{mic}D_{mic}\phi_{mic}}{p_a Z_{mic}}\frac{p_{mic}}{p_a}\rho_{ga}(p_{mac} - p_{mic}) + \rho_{ga}\rho_{shale}\alpha_{mic}D_{mic}\left(\frac{V_{mac-L}p_{mac}}{P_{mac-L} + p_{mac}} - \frac{V_{mic-L}p_{mic}}{P_{mic-L} + p_{mic}}\right) \tag{A-17}$$

where α_{mic} is the shape factor of the micropore, the first term on the right represents the mass exchange equation for free gas, and the second term on the right represents the mass exchange equation for adsorbed gas.

AUTHOR INFORMATION

Corresponding Authors

Yuling Tan − *Department of Engineering Mechanics and Hebei Key Laboratory of Mechanics of Intelligent Materials and Structures, Shijiazhuang Tiedao University, Shijiazhuang 050043, China;* orcid.org/0000-0001-9446-9069; Email: yulingtan@126.com

Zhejun Pan − *Key Laboratory of Continental Shale Hydrocarbon Accumulation and Efficient Development, Ministry of Education, Northeast Petroleum University, Daqing, Heilongjiang 163318, China;* orcid.org/0000-0002-7292-630X; Email: Zhejun.Pan@nepu.edu.cn

Authors

Lingjie Yu − *State Key Laboratory of Shale Oil and Gas Enrichment Mechanisms and Effective Development, Wuxi 214151, China; SINOPEC Key Laboratory of Petroleum Accumulation Mechanism, Wuxi 214151, China; Wuxi Research Institute of Petroleum Geology, SINOPEC, Wuxi 214151, China*

Ming Fan − *State Key Laboratory of Shale Oil and Gas Enrichment Mechanisms and Effective Development, Wuxi 214151, China; SINOPEC Key Laboratory of Petroleum Accumulation Mechanism, Wuxi 214151, China; Wuxi Research Institute of Petroleum Geology, SINOPEC, Wuxi 214151, China*

Ershe Xu − *State Key Laboratory of Shale Oil and Gas Enrichment Mechanisms and Effective Development, Wuxi 214151, China; SINOPEC Key Laboratory of Petroleum Accumulation Mechanism, Wuxi 214151, China; Wuxi Research Institute of Petroleum Geology, SINOPEC, Wuxi 214151, China*

Guanglei Cui − *Key Laboratory of Ministry of Education on Safe Mining of Deep Metal Mines, Northeastern University, Shenyang 110004, China;* orcid.org/0000-0002-9698-8804

Complete contact information is available at: https://pubs.acs.org/10.1021/acsomega.2c02397

Notes

The authors declare no competing financial interest.

ACKNOWLEDGMENTS

The authors acknowledge the financial support from the National Natural Science Foundation of China (42072156, 41690133), the Important National Science & Technology Specific Projects (2017ZX05036-002), and the Sinopec Research Project (P15165).

NOMENCLATURE

t_{des}time of the beginning of gas desorption (s)
$t_{surface}$time of the sample arriving at the wellhead (s)
$t_1$time of applying a second desorption temperature (s)
t_{over}time of the ending of desorption (s)
$p_0$initial gas pressure (Pa)
$p_a$standard atmosphere (Pa)
p_{mud}mud pressure at depth H in the well (Pa)
p_{mac}gas pressure in the macropore (Pa)
p_{mic}gas pressure in the micropore (Pa)
T_{mud}mud temperature (K)
$T_1$the first desorption temperature (K)
$T_2$the second desorption temperature (K)
D_{mac0}gas diffusivity in the macropore in the initial state (m^2/s)
D_{mac}gas diffusivity in the macropore (m^2/s)
D_{mic0}gas diffusivity in the micropore in the initial state (m^2/s)
D_{mic}gas diffusivity in the micropore (m^2/s)
J_{mac}gas flow flux in the macropore ($kg/(m^2*s)$)
J_{mic}gas flow flux in the micropore ($kg/(m^2*s)$)
$Q$the commutative term of the macropore and the micropore ($kg/(m^3*s)$)
$m_{mac\text{-}ads}$the mass of the adsorbed gas per unit volume in the macropore (kg/m^3)
$m_{mac\text{-}ads0}$the mass of the adsorbed gas per unit volume in the macropore in the initial state (kg/m^3)
$m_{mac\text{-}free}$the mass of the free gas per unit volume in the macropore (kg/m^3)
$m_{mac\text{-}free0}$the mass of the free gas per unit volume in the macropore in the initial state (kg/m^3)
$m_{mic\text{-}ads}$the mass of the adsorbed gas per unit volume in the micropore (kg/m^3)
$m_{mic\text{-}ads0}$the mass of the adsorbed gas per unit volume in the micropore in the initial state (kg/m^3)
$m_{mic\text{-}free}$the mass of the free gas per unit volume in the micropore (kg/m^3)
$m_{mic\text{-}free0}$the mass of the free gas per unit volume in the micropore in the initial state (kg/m^3)
ϕ_{mac}porosity of the macropore (-)
ϕ_{mic}porosity of the micropore (-)
Z_{mac}gas compression factor of the macropore (-)
Z_{mic}gas compression factor of the micropore (-)
ρ_{ga}density of gas at standard condition (kg/m^3)
ρ_{shale}density of shale (kg/m^3)

https://doi.org/10.1021/acsomega.2c02397
ACS Omega 2022, 7, 21246−21254

$V_{mac\text{-}L}$Langmuir volume constant in the macropore (m^3/kg)
$P_{mac\text{-}L}$Langmuir pressure constant in the macropore (Pa)
$V_{mic\text{-}L}$Langmuir volume constant in the micropore (m^3/kg)
$P_{mic\text{-}L}$Langmuir pressure constant in the micropore (Pa)
α_{mic}Shape factor of the micropore (m^{-2})

REFERENCES

(1) Aydin, G.; Karakurt, I.; Aydiner, K. Analysis and mitigation opportunities of methane emissions from energy sector. *Energy Sources, Part A* **2012**, *34*, 967−982.
(2) Guo, X.; Marinova, D.; Hong, J. China's Shifting Policies towards Sustainability: a low-carbon economy and environmental protection. *J. Contemporary China* **2013**, *22*, 428−445.
(3) Tan, Y.; Pan, Z.; Feng, X.; Zhang, D.; Connell, L. D. Laboratory characterisation of fracture compressibility for unconventional gas reservoir rocks: A review. *Int. J. Coal Geol.* **2019**, *204*, 1−17.
(4) Li, K.; Meng, Z.; Ji, J.; Zheng, X.; Zhang, Q.; Zou, W. Characteristics and influencing factors of desorption gas in Wufeng-Longmaxi formations in Fuling area Sichuan Basin. *Pet. Geol. Exp.* **2018**, *40*, 90−96.
(5) Shi, W.; Wang, X.; Zhang, C.; Feng, A.; Huang, Z. Experimental study on gas content of adsorption and desorption in Fuling shale gas field. *J. Pet. Sci. Eng.* **2019**, *180*, 1069−1076.
(6) He, L.; Mei, H.; Hu, X.; Dejam, M.; Kou, Z.; Zhang, M. Advanced flowing material balance to determine original gas in place of shale gas considering adsorption hysteresis. *SPE Reservoir Eval. Eng.* **2019**, *22*, 1282−1292.
(7) Yao, G.; Wang, X.; Du, H.; Yi, W.; Guo, M.; Xiang, R.; Li, Z. Applicability of USBM method in the test on shale gas content. *Acta Petrolei Sinica* **2016**, *37*, 802−806.
(8) Zhang, X.; Shi, W.; Shu, Z.; Xu, Z.; Wang, C.; Yuan, Q.; Xu, Q.; Wang, R. Calculation Model of Shale Gas Content and Its Application in Fuling Area. *Earth Sci.* **2017**, *42*, 1157−1168.
(9) Dong, Q.; Liu, X.; Dong, Q.; Li, W. Determination of gas content in shale. *Nat. Gas Oil* **2012**, *30*, 34−37.
(10) Xi, C.; Sun, C.; Fang, F.; Shu, X.; Wang, Q.; Zhang, L. Field testing technology for shale gas content. *Pet. Geol. Exp.* **2018**, *40*, 25−29.
(11) Qin, X. Analysis on determination method of lost gas in shale gas content. *Underground Water* **2015**, *37*, 231−232.
(12) Liu, G.; Zhao, Q.; Gao, C.; Jiang, L.; Sun, J.; Liu, C. A critical desorption time method to improve the calculation accuracy of gas loss in shale gas content testing. *Nat. Gas Ind.* **2019**, *39*, 71−75.
(13) Zhang, J.; Liu, Z.; Li, L. Use and improvement of the desorption method in shale gas content tests. *Nat. Gas Ind.* **2011**, *31*, 108−112.
(14) Bertard, C.; Bruyet, B.; Gunther, J. Determination of desorbed gas concentration of coal (direct method). *Int. J. Rock Mech. Min.* **1970**, *7*, 43−65.
(15) Kissell, F. N.; McCulloch, C. M.; Elder, C. H. *Direct method of Determining Methane Content of Coalbeds for Ventilation Design*, U.S. Department of the Interior Bureau of Mines Ri: Pittsburgh PA, 1973.
(16) Smith, D. M.; Williams, F. L. *New Technique for Determining The Methane Content of Coal, American Society of Mechanical Engineers 16th Intersociety Energy Conversion Engineering Conference*, 1981.
(17) Smith, D. M.; Williams, F. L. Diffusion models for gas production from coal:determination of diffusion parameters. *Fuel* **1984**, *63*, 256−261.
(18) Wei, Q.; Yan, B.; Xiao, X. Research progress on the desorption methods of shale gas. *Nat. Gas Geosci.* **2015**, *26*, 1657−1665.
(19) Metcalfe, R. S.; Yee, D.; Seidle, J. P.; Puri, R. Review of research efforts in coalbed methane recovery *SPE* 1991, *23025*.
(20) Yee, D.; Seidle, J. P.; Hanson, W. B. Gas sorption on coal and measurement of gas content. *AAPG Studies in Geology* **1993**, *38*, 203−218.
(21) Hao, J.; Jiang, Z.; Xing, J.; Li, Z.; Tang, X.; Su, J. An Improved M ethod of Calculating Lost Gas Content of Shale Gas. *Geosci. J.* **2015**, *29*, 1475−1482.
(22) Lu, M.; Pan, Z.; Connell, L. D.; Lu, Y. A New Method for the Estimation of Lost Gas during the Measurement of the Gas Content of Coal, *SPE Asia Pacific Unconventional Resources Conference and Exhibition*,2015.
(23) Fan, Z.; Zhang, Q.; Lu, X.; Luo, W. Analysis on gas lost content of coalbed methane and influenced factors. *Int. J. Coal Sci. Techn.* **2010**, *38*, 104−108.
(24) Shtepani, E.; Noll, L. A.; Elrod, L. W.; Jacobs, P. M. A new regression-based method for accurate measurement of coal and shale gas content. *SPE Reserv. Eval. Eng.* **2010**, *13*, 359−364.
(25) Song, J.; Su, X.; Wang, Q.; Chen, P. A new method for calculating gas content of coal reservoirs with consideration of a micro-pore over pressure environment. *Nat. Gas Ind.* **2017**, *37*, 182−188.
(26) Waechter, N. B.; Hampton, G. L.; Shipps, J. C. Overview of Coal and Shale Gas Measurement:field and Laboratory Procedure, *Proceedings of 2004 International Coalbed Methane Symposium, Tuscaloosa, USA*, 2004.
(27) Tao, S.; Chen, S.; Pan, Z. Current status, challenges, and policy suggestions for coalbed methane industry development in China: A review. *Energy Sci. Eng.* **2019**, *7*, 1059−1074.
(28) Chen, T.; Feng, X.; Cui, G.; Tan, Y.; Pan, Z. Experimental study of permeability change of organic-rich gas shales under high effective stress. *J. Nat. Gas Sci. Eng.* **2019**, *64*, 1−14.
(29) Xue, X.; Yue, X.; Wei, W. Some Suggestions in Shale Gas Content Measuring Process. *Coal Geol. China* **2013**, *25*, 27−29.
(30) Lu, M.; Pan, Z.; Connell, L. D.; Lu, Y. A coupled, non-isothermal gas shale flow model: Application to evaluation of gas-in-place in shale with core samples. *J. Pet. Sci. Eng.* **2017**, *158*, 361−379.
(31) Yu, L.; Fan, M.; Jiang, Q.; Tang, Q.; Zhang, W.; Shu, X. Optimization of shale gas desorption method in field. *Pet. Geol. Exp.* **2015**, *37*, 402−406.
(32) Liu, H.; Yan, G.; Li, X. *Measurement Method of Shale Gas Content*; Petroleum Industry Press: Beijing, 2014.
(33) Pan, Z.; Connell, L. D.; Camilleri, M.; Connelly, L. Effects of matrix moisture on gas diffusion and flow in coal. *Fuel* **2010**, *89*, 3207−3217.
(34) Yuan, W.; Pan, Z.; Li, X.; Yang, Y.; Zhao, C.; Connell, L. D.; Li, S.; He, J. Experimental study and modelling of methane adsorption and diffusion in shale. *Fuel* **2014**, *117*, 509−519.
(35) Ma, Y.; Pan, Z.; Zhong, N.; Connell, L. D.; Down, D. I.; Lin, W.; Zhang, Y. Experimental study of anisotropic gas permeability and its relationship with fracture structure of Longmaxi Shales, Sichuan Basin, China. *Fuel* **2016**, *180*, 106−115.
(36) Cui, G.; Liu, J.; Wei, M.; Feng, X. T.; Elsworth, D. Evolution of permeability during the process of shale gas extraction. *J. Nat. Gas Sci. Eng.* **2018**, *49*, 94−109.
(37) Pan, Z.; Ma, Y.; Connell, L. D.; Down, D. I.; Camilleri, M. Measuring anisotropic permeability using a cubic shale sample in a triaxial cell. *J. Nat. Gas Sci. Eng.* **2015**, *26*, 336−344.
(38) Tan, Y.; Pan, Z.; Liu, J.; Kang, J.; Zhou, F.; Connell, L. D.; Yang, Y. Experimental study of impact of anisotropy and heterogeneity on gas flow in coal. Part I: Diffusion and adsorption. *Fuel* **2018**, *232*, 444−453.
(39) Wang, J.; Kabir, A.; Liu, J.; Chen, Z. Effects of non-Darcy flow on the performance of coal seam gas wells. *Int. J. Coal Geol.* **2012**, *93*, 62−74.

https://doi.org/10.1021/acsomega.2c02397
ACS Omega 2022, 7, 21246−21254